

# Parameters of Tomonaga-Luttinger liquid in a quasi-1D material with Coulomb interactions

Piotr Chudzinski

*School of Mathematics and Physics, Queen's University of Belfast*

(Dated: 02.02.2020)

In this work we derive a new scheme to calculate Tomonaga-Luttinger liquid (TLL) parameters and holon (charge modes) velocities in a quasi-1D material that consists of two-leg ladders coupled through Coulomb interactions. Firstly, we obtain an analytic formula for electron-electron interaction potential along the conducting axis for a generalized charge distribution in a plane perpendicular to it. In the second step we introduce many-body screening that is present in a quasi-1D material. To this end we propose a new approximation for the charge susceptibility. Based on this we are able to find the TLL's parameters and velocities. We then show how to use these to validate the experimental ARPES data measured recently in p-polarization in  $NbSe_3$ . Although we focus our study on this specific material it is applicable for any quasi-1D system that consists of two-leg ladders as basic units.

PACS numbers:

Probing spin-charge separation in quasi-1D materials has been one of the long-standing challenges in experimental solid state physics of strongly correlated systems. More than two decades<sup>1</sup> of attempts has produced more false alarms than proper findings and, as a result, most recent experimental evidences are combined with a theoretical estimate of e.g. TLL collective modes' velocities<sup>2,3,4</sup>. A strong emphasis is then put on the fact that the experiment and theory are in a reasonable quantitative agreement. While such procedure has been outlined for a Hubbard-like models, with short range interactions, there is no such a scheme available for other class of realizations, actually more frequent, i.e. systems with long range interactions. This work aims to fill this gap, and to do it by providing analytical expressions for the desired quantities, which, contrary to numerical results, are easily transferable from one case to another. So far, among these class of models, only carbon nanotubes were investigated in detail, see seminal work Ref.<sup>5</sup>, here we extend this work to apply it to systems with lower local symmetry.

The successful search for the TLL is facing two conditions i) and ii). The frequently used model with a short range Hubbard U-V interactions is valid for a quasi-1D material where the other 2D (or 3D) bands, that are not crossing Fermi energy  $E_F$  but provide screening, fall very close enough (a fraction of a bandwidth) to the  $E_F$ . However, the opposite situation is more frequent, where the other bands overlap (in energy) only with the very bottom of the 1D band i). This gives an energy window of a weak screening. Secondly, i), a narrow wire (on atomic scale) that hosts only a single 1D channel is very prone to undergo Peierls instability that destroys the TLL phase. This tendency can be minimized for a larger conduction band electrons' orbital, spread over a few atoms in a unit cell, but then a local symmetry of the orbital will be lowered. The two leg ladder will then be the simplest, and actually the most common, case. This is the situation that we aim to tackle in this paper.

Our study is motivated by a recent experimental report, Ref.<sup>6,7</sup>, of 1D TLL states observed in p-pol in  $NbSe_3$ . We can summarize those findings as: i) at each Fermi point there are *two* linear dispersions, at the inner band (we shall call this anti-bonding band b1 hence Fermi point  $k_{F1}$ ) the two velocities converge to the same value, at outer band b3 the two velocities are different (one is equal to those at  $k_{F1}$  while the other is a factor  $\approx 1.25$  larger) ii) there is a power law decay of spectral function with  $\alpha = 0.24$ . It is surprising that with such a small ratio of velocities there is such a substantial value of  $\alpha$  exponent and our aim here is to explain this experimental finding.

The manuscript is organised as follows. We start by computing Coulomb interactions potential for a low symmetry 1D column where only the  $C_2$  symmetry operation is presumed. With this we compute the TLL parameters for a single column and for the entire quasi-1D material with partial screening incorporated in the solution. Then we focus on a concrete realisation and analyse the result of ARPES experiment<sup>6,7</sup>.

a. *Tomonaga-Luttinger liquid* The Hamiltonian of the TLL state is written in terms of fluctuations of these collective modes:

$$H^{1D}[\nu] = \sum_{\nu} \int \frac{dx}{2\pi} \left[ (v_{\nu} K_{\nu})(\pi \Pi_{\nu})^2 + \left( \frac{v_{\nu}}{K_{\nu}} \right) (\partial_x \phi_{\nu})^2 \right] \quad (1)$$

where  $\nabla \phi_{\nu}(x)$  gives the local density of fluctuation  $v_{\nu}, K_{\nu}$  are velocity and TLL parameter ( $\sim$ compressibility) of a given bosonic mode  $\nu$ , these depend on electron-electron interactions with small momentum exchange. In the simplest approximation  $v_{\nu} \approx V_F(1 + 2g)$  where  $g$  is a strength of the Coulomb interaction and  $V_F$  is a Fermi velocity  $\sim 2t_b$  (where we take tight binding model with 1D chains arranged along the b-axis) which is  $\sim \Lambda$  (which determines the UV cut-off of our theory). In this paper we aim to improve this simple, approximate formula for  $v_{\nu}$ .

The theory that we derive below can give stringent con-

ditions for the velocities of these collective modes. When the crystal's columns, on which the gapless states exist, are grouped into pairs and so there are two bands crossing Fermi energy then a two leg ladder description applies. Then there are four bosonic modes  $\rho_{\pm}, \sigma_{\pm}$  as both spin and charge can oscillate symmetrically or anti-symmetrically within the two legs of the ladder, we call it later total and transverse modes respectively. In other words total mode is a density fluctuation simultaneously in both legs, while transverse mode is a density fluctuations in opposite way in two legs of the ladder. The first step, in quantitative treatment of Coulomb interactions, is to find their dependence as a function of inter-carriers' distance.

*b. Single ladder* We build our reasoning on the top of some single-particle DFT calculations, which presumably provides us with electronic density of the carriers occupying the 1D band. What such calculations are unable to capture are electron-electron correlations inevitably present in 1D many-body state described by Eq.1. We seek a way to determine  $v_{\nu}, K_{\nu}$  from the knowledge of single-particle physics. If we assume that for each separate ladder the charge density is spread over a section of a distorted toroid then the bare Coulomb potential reads<sup>5</sup>

$$\bar{V}_{\text{Coul}}(\vec{r}-\vec{r}') = \frac{e^2/\kappa}{\sqrt{(x-x')^2 + 4R^2 \sin^2((y-y')/2R) + d_z^2}} \quad (2)$$

where the  $d_z$  is a thickness of the toroid. The scattering amplitude (that enters to second quantization Hamiltonian) of the Hartree type interaction is given by an integral over the elementary unit cell:

$$V(\vec{r}, \vec{r}') = \int d\vec{r} \Psi^*(\vec{r}) \Psi^*(\vec{r}') \bar{V}_{\text{Coul}}(\vec{r}-\vec{r}') \Psi(\vec{r}) \Psi(\vec{r}') \quad (3)$$

where  $\Psi^*(\vec{r}), \Psi(\vec{r}')$  are wave-functions of interacting electrons, a Bloch waves along the x-direction and in a perpendicular plane a section of a toroid of a given thickness. We add an extra parameter  $\zeta$  that accounts for an inhomogeneity along the circumference of the toroid where  $\zeta = 0$  correspond to the symmetric homogeneous distribution (or constant radius) like in nanotube. Hence we shall generalize expression given in Ref.<sup>5</sup> for symmetric CNT. We integrate over perpendicular coordinates to get an interaction amplitude along the b-axis  $V(x)$ :

$$V(x) = \int_{\phi_R}^{2\pi R} \int_{\phi_R}^{2\pi R} \frac{dy}{2\pi R} \frac{dy'}{2\pi R} \frac{\bar{V}_{\text{Coul}}(\vec{r}-\vec{r}')}{1 - \zeta \sin((y-y')/2R)} \quad (4)$$

The closed analytic form for the integral is known also in this more general case:

$$V(x) = \bar{U} \frac{\sqrt{1 - \zeta^2} \Pi \left( \phi; \zeta \left| \left( \frac{2R}{\sqrt{d^2 + 4R^2 + (x-x')^2}} \right)^2 \right. \right)}{\left( \phi \sqrt{d^2 + 4R^2 + (x-x')^2} \right)} \quad (5)$$

where  $\Pi(\phi; \zeta | 1/\tilde{x})$  is the incomplete elliptic integral of the third kind. The integral is parametrized by  $\bar{U} = U/N$  (chosen appropriately depending on the ab-initio method) e.g. for cRPA we account for all screening provided by carriers residing on all other orbitals but not the 1D d-orbital. The parameters  $\phi$  (angle of the sector of the toroid) and  $\zeta$  (distortion of the toroid) are determined by the geometry of the given *eigen-orbital* in the a-c plane perpendicular to 1D axis. The prefactor ensures that no matter what the geometry, there total density of charge is normalized. At a given UV cut-off  $\Lambda$  (usually equal to the lattice spacing) the interaction saturates to a value given by local Hubbard-type repulsion. For the case of Nb atom we use the following cRPA value<sup>8</sup>  $U = 2.8eV$  which, with  $N=3$  (to account for a partial occupancy of Se sites in  $\text{NbSe}_3$ ), sets the amplitude of electron-electron interactions. We need to perform Fourier transform of  $V(x)$  which will complete our description of the Hartree term in a single ladder/column.

For Coulomb electron-electron interactions there shall be also exchange interactions. Their value, for  $r = a$  is again known from the *ab-initio* calculations and parametrized by  $J(r = a) = J$  which in the case of  $\text{NbSe}_3$  is  $J = 0.6eV$ . This can be thought of as an interaction of a carrier with an exchange hole of another carrier. The exchange hole is described by a two-body correlation function  $g(x, x')$ . This extra term will convolve one of the wave-functions in Eq.3. The two-body density, in a translationally invariant TLL, has a dominant contribution that scales like  $(r - r')^{-(1/4(1/K+3/K_s)+2)}|_{K_s=1}$ .

For sufficiently strong repulsive interactions, we obtain a quantity that rapidly decays in real space which agrees well with our intuitive understanding of exchange. Then the overall Fourier transform  $J(q)$  will be the previous Fourier transform of screened Coulomb potential times an increasing power law and so the  $J(q = 2k_F)$  may be substantial (please note that this enters only to  $g_2$  and does not enter to backscattering terms  $g_1$ ).

*c. Quasi-1D material* After we have established the parameters of a single ladder, we shall now move on to a quasi-1D material – a system that consist of multitude of parallel ladders. The full modelling has to account for the fact that we are dealing with a set of 1D systems coupled by long range density-density (forward scattering) interactions, these inter-ladder (charge) density-density terms are non-negligible, they can be as large as  $t_b/2$ . We first compute screening of single TLL by other columns which cuts the divergence  $V(q)$  when  $q \rightarrow 0$ . To this end we take  $V_{eff}(q) = V(q)/(1 + G(q, T)\chi_{TLL}(q))$ . Here we take an RPA approximation for the dielectric function. For the charge susceptibility of the two leg ladder with one velocities much different than  $V_F$  and all other velocities  $v_{\rho-, \sigma_{\pm}} \approx V_F$  (see below) and  $K_{\rho-, \sigma_{\pm}} \approx 1$  we can generalize the result obtained in Ref.<sup>9</sup>

$$\chi_{TLL}(q) = 4\pi \frac{\Gamma\left(1 - \left(\frac{K_{\rho+}}{4} + \frac{3}{8}\right)\right)}{\Gamma\left(\frac{K_{\rho+}}{4} + \frac{3}{8}\right)} \frac{|\omega^2 - V_F^2 q^2|^{\left(\frac{K_{\rho+}}{4} + \frac{3}{8}\right)-1}}{V_F^{\left(\frac{K_{\rho+}}{4} + \frac{3}{8}\right)-1}} \exp\left(-i\pi\left[\left(\frac{K_{\rho+}}{4} + \frac{3}{8}\right) - 1\right]\mathfrak{H}_\Theta[\omega^2 - V_F^2 q^2]\right) F_1\left(\frac{K_{\rho+}}{4}, \frac{K_{\rho+}}{4} + \frac{3}{8} - \frac{1}{2}, 1 - \left(\frac{K_{\rho+}}{4} + \frac{3}{8}\right), \frac{K_{\rho+}}{4} + \frac{3}{8}; 1 - \left(\frac{v_{\rho+}}{V_F}\right)^2, 1 - \frac{\omega^2 - v_{\rho+}^2 q^2}{\omega^2 - v_F^2 q^2}\right) \Big|_{\omega \rightarrow \Lambda_{IR}} \quad (6)$$

where  $F_1()$  is the Appell hypergeometric function and  $\mathfrak{H}_\Theta$  is a Heaviside theta function that appears upon analytic continuation. For the  $G(q, T)$ , which accounts for a local field corrections we take  $G(q, T) = \bar{G}(q, T)/(q^2 + \Lambda_{IR}^2)$  which is a screened Coulomb interaction times the static structure factor, the lesser correlation function of the screening medium (it is by definition what local field correction is supposed to capture). We take  $\bar{G}(q, T) \sim A(q, \omega \rightarrow 0, T; \Delta \equiv \Lambda_{IR})$  where the spectral function is known from Ref.<sup>10</sup> and the IR cut-off  $\Lambda_{IR} = \max(T, t_\perp)$ . Please note that with this choice the entire  $G(q, T)$  can be interpreted as a propagator (i.e. a retarded correlation function in the Lehmann representation) of the bosons (the holons) carrying interactions in between the 1D wires. Here we used the fact that the sole 1D ladder cannot self-screen itself (and RPA expression is exact therein, local field corrections are absent) so entire local field correction must originate from its environment. This approach, based on the  $t_\perp$  tunnelling, is sufficient to limit the increase of  $V_{eff}(q \rightarrow 0)$  to a well defined constant value, which among other implication also gives a finite, non-divergent holon's velocity.

We can now proceed with the quantitative estimate of the TLL parameters  $K_\nu$  in Eq.1 for the two leg ladder. The bosonization is made in  $0/\pi$  bands so one begins with Hartree and Fock intra and inter-band interactions. In each band we have Hartree  $V(q)$  and Fock  $J(q)$  and then it is known<sup>11</sup> that:

$$\begin{aligned} g_{4mn} &= 1/2(2V^{(mn)}(q=0) - J^{(mn)}(q=0))/\sqrt{V_{Fm}V_{Fn}} \\ g_{2mn} &= ([V^{(mn)}(q=0) + J^{(mn)}(q=2k_{Fo/\pi})] \\ &- 1/2[V^{(mn)}(q=2k_{Fo/\pi}) + J^{(mn)}(q=0)])/\sqrt{V_{Fm}V_{Fn}} \\ g_{\sigma mn} &= -J^{(mn)}(q=0)/\sqrt{V_{Fm}V_{Fn}} \quad (7) \end{aligned}$$

where  $m, n = o, \pi$  and we took into account a possibility of different Fermi velocities in both bands. The band dependence of interaction comes from their different shapes. We performed Fourier transforms of Eq.5 numerically (screening is independent on the band index) to find that  $V^{\pi\pi} \leq V^{oo}$ . This is because we assumed that in NbSe<sub>3</sub> the bonding orbital is more spread (larger angle  $\phi$ ), thinner and closer to the center (smaller  $R$  and  $d_z$ ). This is compensated by the Fermi velocity difference so  $g_{oo} \approx g_{\pi\pi}$ . The inter-band terms are more complicated to analyse. We assume that product of the two densities is intermediate but also less homogeneous (larger  $\zeta$ )

which results in larger  $V_{o\pi}$ . This is compensated by the following effect: the inter-band Hartree interaction is reduced by a factor  $V_{2o\pi} = J_0((k_{Fo} - k_{F\pi})a)V_{oo}$  (which comes from computing an overlap between two waves of slightly different periodicity: one takes two phase shifted waves and average the phase shift). However the  $J_{o\pi} = 0$  which can be obtained directly by performing integral of the form of Eq.5 over even/odd function or, if we treat band index as pseudo-spin variable, then the  $J_{o\pi}$  is anti-parallel (pseudo-)spin process. One now writes the density-density interactions in a band-basis in a matrix form and performs  $S[\pi/2]$  rotation to total-transverse basis  $g_\nu$ . Since  $g_{oo} \approx g_{\pi\pi} \approx g_{o\pi}$  the  $g_{\rho+}$  is by far the largest, but since it is further modified by inter-chain interactions we discuss it separately below. The TLL parameters and velocities for the neutral modes follow directly from here and can be given by the following, single ladder, formula:  $K_\nu = \sqrt{\frac{1-g_\nu}{1+g_\nu}}$  where  $g_{\rho-} = (g_{2o} - g_{2\pi}) + J_{oo}(2k_F)$ ,  $g_{\sigma+} = g_{\sigma o} + g_{\sigma\pi}$  and  $g_{\sigma-} = g_{\sigma o} - g_{\sigma\pi}$ .

Please note that from the Fourier transforms of our potential we also know that for  $q = 2k_F$   $g_{o\pi} < g_{\pi\pi} \geq g_{oo}$  which (from spin SU(2) symmetry) also implies a hierarchy of the sine-Gordon terms.

*d. Holon mode: Connection with the experimental results* In most general case one expects the following spectrum: four linear dispersions that start at each Fermi point. Two charge modes shall cross at the  $\Gamma$  points (forming structures that each resembles a Dirac point with constant velocities) while two spin modes shall have parabolic behaviour (hence their velocity depends on  $q_{||}$  and  $v_{\sigma\pm}(q_{||} \rightarrow \Gamma) \rightarrow 0$ ) around the  $\Gamma$  point<sup>16</sup>.

As it was proven above, weakly screened interaction which retains predominantly long range character the three modes ( $\sigma\pm$  and  $\rho-$ ) have velocities that are very close to the average Fermi velocity (average from both bands  $(V_{Fb1} + V_{Fb3})/2$  where  $V_{Fb1,3}$  are known from DFT) and so these dispersions are rather close to each other, while the total charge mode ( $\rho+$ ) velocity is noticeably larger. It is because: 1) the difference between DFT bands' velocities  $\Delta v$  is irrelevant in RG sense and hence it goes to zero as we approach the Fermi level; 2) in bosonic language when at  $q \rightarrow 0$  the  $g_{oo} \approx g_{\pi\pi} \approx g_{o\pi}$  only the  $\nabla\phi_{\rho+}$  operator is coupled with the long range interactions; 3) we are not in the situation of interactions coupled ladders where  $K_{\rho\pm}$  are determined through a split of single leg  $K_\rho$ . This is invalidated by strong hybridization

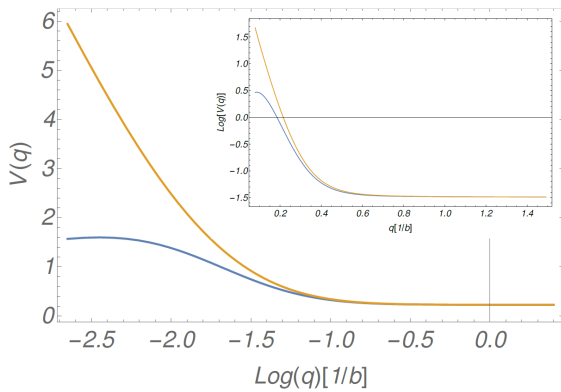
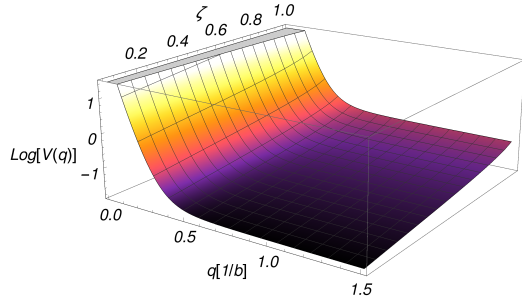


FIG. 1: Top panel: Fourier transform of the Coulomb interaction Eq.5 shown as a function of momentum and parameter  $\zeta$  that describes inhomogeneity (eccentricity) of the cross-section. Bottom panel: Screening effects. Logarithm of electron-electron interactions as a function of momentum  $q$ . Yellow curve is for bare non-screened  $V_{Coul}(q)$ , a Fourier transform of Eq.5, while blue line is screened by the susceptibility given in Eq.6. The main plot is in log-linear coordinates and manifest the asymptotic  $\sim \text{Log}(q)$  behaviour while the inset is in linear-log coordinates to show the real momentum dependence.

on the rungs (relevant in RG sense), that leads to large split between DFT bonding and anti-bonding band, the transverse modes can be rewritten as pseudo-spins with large gap between pseudo-singlet and pseudo-triplet excitations.

Now we account for the finite aperture size of ARPES, which implies that the final state is a mixture of waves with different  $q_{\perp}$  (this is a coherent state that results from Fresnel diffraction of electronic waves<sup>12</sup>) The problem is simplified because again only  $\rho+$  modes are exposed to these long-range interactions. The treatment of this system can then be based directly on the solution provided by H.J.Schulz in Ref.<sup>13</sup>. In that work it was found that the velocity is equal to:

$$v_{\rho+} = \int_0^{\Delta q_{\perp}} dq_{\perp} V_F \sqrt{[(1 + g_{40})^2 - 4g_{20}^2] + \frac{g_{\perp}}{(\epsilon_{\parallel}^{(0)}(1 + \epsilon_{\perp}^{(0)}(q_{\parallel}/q_{\perp})^2)}(1 + 2g_{40} - 2g_{40})} \quad (8)$$

where  $g_{\perp} = V_{\perp}/V_F$ ,  $g_{40} = \sum g_{4mn}$  and we took a slightly different limit than in Ref.<sup>13</sup>, since here we are interested in  $q_{\parallel} \rightarrow 0$  limit (in an under-screened 1D model<sup>17</sup>) and at the same time we take an integral over finite  $q_{\perp}$  in order to account for the finite aperture of the (Fresnel zone

focused) nanoARPES device. At the same time the exponent of the single particle Green's function (momentum integrated) is equal to  $\alpha = (C_{\rho+} + C_{\rho+}^{-1})/8 + 6/8 - 1$  where  $6/8$  comes from the three bosonic modes with  $K_{\nu} \approx 1$  and:

$$C_{\rho+} = \sqrt{\frac{1+2g_{40}-2g_{20}}{1+2g_{40}+2g_{20}}} \left(1 + \frac{\pi}{8} \frac{g_{\perp}}{1+2g_{40}+2g_{20}} \ln\left[\frac{g_{\perp}}{4(1+2g_{40}+2g_{20})}\right]\right) \quad (9)$$

The above formulas, with a physically sensible  $g_{\perp} \in (0.4, 0.6)$  gives the following estimates for observable quantities  $v_{\rho+} \in (1.2, 1.35)V_F$  and  $\alpha \in (0.15, 0.2)$ .

*e. Relative intensity of the four modes* The formula Eq.5 allows not only to compute parameters of stationary TLL, but also to study the dynamics of an excited photo-hole. This in turn gives an insight into relative intensities measured for various TLL modes. To investigate the relative intensities of the four bosonic dispersions we take the three step model for photo-emission. Contrary to the Fermi liquid, in TLL for each momenta we have several (four in our case) bosonic branches and the strength of each relaxation channel is proportional to an overlap integral between a photo-density  $\rho_i(\vec{r})$  (defined below) and a given collective excitation of TLL. Initially, just after the photo-emission event, the photo-hole (a single fermion state) is created in an intermediate state  $\psi_i(\vec{r})$  that is not an eigenstate but rather a local combination of many excited states of the system. Then this initial excitation relaxes into collective, bosonic eigen-states of the many-body system. The relaxation is slower than for the single-particle bands and happens through Coulomb interaction<sup>14</sup>, the one given in Eq.5, i.e.

$$H_{rel} = T(1, 2)\rho(q, \omega)c_{bi}(k_F)c_i^{\dagger}(k_{phot}) \quad (10)$$

where we annihilate the photo-hole by taking an electron from the Fermi surface, these are the last two annihilation-creation operators in the above formula and can be together called the *photo-density*  $\rho_i(\vec{r}) \equiv$  an *electron-intermediate* hole  $c(k_F)c_i^{\dagger}(k_{phot})$ . The energy-momentum created in this decay process goes into a particle-hole density excitation, an eigen-state of the TLL, through electron-electron interaction  $T_{1,2} \sim V_{eff}(x)$ . The  $\psi_i(\vec{r})$  is located on atomic orbitals that fulfil dipole matrix ARPES selection rules and among these has to have a spatial distribution matching the evanescent wave of the emitted photo-electron, to ensure their large overlap. The photo-electron wave-function can be computed by inverse scattering method<sup>12</sup> and from this calculation we know that  $\psi_i(r_{\perp}) \approx H_0(r_{\perp})$  inside the 1D wire (that acts as a trap). Since the Hermite polynomial  $H_0(r_{\perp})$  is a symmetric Gaussian then the overall symmetry of  $\rho_i(r_{\perp})$  is determined by a wave-function of the  $c_{bi}(k_F)$  i.e.  $\psi_{b1,3}(\vec{r}; k_{F1,3})$  is a wavefunction (at the Fermi level) of a matching band

The amplitude of the process, when resolved among different bosonic modes, reads:

$$T(1 = i, 2 = \nu) = \int dr_{\perp} V_{eff}(\vec{r})\rho_{\nu}(\vec{r})\psi_i(\vec{r})\psi_{b1,3}(\vec{r}; k_{F1,3}) \quad (11)$$

where the last two terms taken together give  $\rho_i(\vec{r})$  and  $\rho_{\nu}(\vec{r}) = \nabla\phi_{\nu}$ . Different TLL modes have different symmetry with respect to the middle horizontal plane of a two leg ladder: the total modes  $\nabla\phi_{\rho+}, \nabla\phi_{\sigma+}$  describe oscillations in phase of the densities of the two legs of the ladder while the transverse modes  $\nabla\phi_{\rho-}, \nabla\phi_{\sigma-}$  describe oscillations in anti-phase. On the other hand, the difference between the two DFT bands is that one is symmetric (the bonding one b3 in  $NbSe_3$ ) and the other anti-symmetric (anti-bonding one b1 in  $NbSe_3$ ) on the rung that links the two legs of the ladder. Hence we can deduce that  $\rho_i(\vec{r})$ : for  $(\omega, k)$  emission point close to the b3 (bonding band) dispersion  $\rho_i(\vec{r})$  is an electron-hole described as a wave with two legs oscillating in phase, while for  $(\omega, k)$  close to the b1 (anti-bonding) band  $\rho_i(\vec{r})$  is a hole's wave-function with an extra  $\pi$  phase (or a '-' sign) between the two legs of the ladder. Since potential given by Eq.5 is symmetric and does not allow to mix  $(\omega, k)$  points then in the first case relaxation into TLL eigenstates of the total holon/spinon modes is much more probable, while in the second case relaxation into transverse holon/spinon modes is much more probable. Let us emphasize that this selection rule is different from the standard dipole matrix selection rule frequently used in polarization dependent ARPES, also used in  $NbSe_3$ . The latter rule relates polarization vector with final states in the sample *and in the detector*, while in the present case the selection is between several emergent collective solutions of a many-body problem (that all admit some eigen-state at the same  $\vec{q}$ ). Please note that this selection rule is based on the fact that  $V_{eff}(q)$  is strongly decaying with increasing  $q$ .

Overall we predict that at each Fermi point ARPES will detect *two* (instead of four) linear dispersions starting at  $k_{F3}$  and  $k_{F1}$ . The two branches are distinguishable when the dispersion approaches the  $\Gamma$  point of Brillouin zone, since one is linear (charge) and one is parabolic (spin). The velocity of the spinon branch at  $k_{F3}$  (total spin mode) is expected to be equal to velocities of transverse modes visible at  $k_{F1}$ . The holon branch visible at  $k_{F3}$  should have velocity approximately 25% higher than other dispersions.

*f. Discussion* Situation is even more complex if the TLL holon dispersion crosses a single-particle band as it happens e.g. with band b2 in  $NbSe_3$ . Then the photo-hole may relax much faster into these single particle states especially in the vicinity of the crossing point. This shall manifest in experiment since at the crossing with the dispersion of the single electron b2 band we expect that  $\psi_i(\vec{r})$  will sink out into this auxiliary dispersion so the intensity of the bosonic branches will be

diminished. When energy of the photo-hole is larger than that of electrons bound within the band b2, then a two stage process is possible: in the first stage single particle from the b2 falls onto a photo hole state and later the b2 hole relaxes onto Fermi level producing the final bosonic excitation  $1_i \rightarrow 1_{b2+\nu} \rightarrow 2_\nu$ . This is a higher order process with two *intermediate*  $e$ - $h$  involved, but it may be favoured by faster b2 relaxation rate. Then the selection rule described above does not apply any more, instead the amplitude is proportional to  $T(1_i, 1_{b2+\nu}, 2_\nu)$ . Experimentally this recovery of  $\rho+$  mode intensity in the anti-symmetric band (e.g. b1 in NbSe<sub>3</sub>) will manifest as an emergence of a second, shifted Dirac cone ( $\approx 0.1\text{eV}$  below the bottom of the  $\rho-$  cone) with a velocity  $v_{\rho+}$  hence substantially larger than  $V_F$ . This is precisely what has been observed in the experiment, Ref.<sup>6,7</sup>.

Finally, we note that in Eq.10 we took a simplified picture of a photohole releasing entire excess energy in one column, while in Eq.8 we took a model of a photohole that creates extra electron-hole pairs in other columns. They provide screening, absorb finite  $q_\perp$  in a coherent manner and constructively interfere with the main wavefunction as proven by geometric series re-summation in Ref.<sup>12</sup>. All these processes, mediated by  $V_{eff}(q)$ , should increase the amplitude of the process when photo-hole momentum is small. Such increase of intensity is indeed observed in Ref. and this validates our approach in the Eq.8.

It is worth noting, that with small modifications, result of current work can be also applied to systems that are recently under intense scrutiny: artificial 1D systems created (or self-organized) on a dielectric surface. On a surface the interactions are substantially less screened, hence the necessity to tackle the system of electrostatically

coupled wires with strong  $g_\perp$  and weak  $t_\perp$ . Here it has to be noted that our approach is complementary to the in Ref.<sup>15</sup> where they have modelled a single wire of a substantial perpendicular size (a mesoscopic effective charge density with perpendicular decay length long on the atomistic scale). However attempts to bring such a mesoscopic model to sub-nm domain, while neglecting entire atomic/orbital physics, has to be excluded as unreliable and our microscopic approach offers a much better approximation in this case. The transverse size of the 1D system can be extracted e.g. from STM measurements while exact geometry of the system, even in the case of corrugated domain edges in 2D topological insulator, can be found from Fourier transforms along the domains and perpendicular to it, so all the data are in principle accessible.

In conclusion we have given a closed analytic expression for density-density interactions in quasi-1D materials. With input parameters known from DFT calculations, such as conduction orbital shape and strength of local interaction (effective Hubbard  $U$  e.g. from cRPA), one is able to give the value of the TLL parameter for the holon modes. We also analyse in detail the outcome of the recent ARPES experiment. For concreteness, we apply our results to a recently studied material NbSe<sub>3</sub>, however our reasoning presented here, can serve as a benchmark for future ARPES studies of similar quasi-1D compounds.

*Acknowledgements* I would like to sincerely thank Thierry Giamarchi, Marco Grioni, Stephane Pons and Miguel A. Valbuena for numerous discussions that inspired this study and, in particular, Enric Canadell for sharing his vast knowledge on quasi-1D materials.

<sup>1</sup> R. Claessen, G.-H. Gweon, F. Reinert, J.W. Allen, W.P. Ellis, Z.X. Shen, C.G. Olson, L.F. Schneemeyer, and F. Lvy. Angle-resolved photoemission of quasi-one-dimensional metals: Evidence for luttinger liquid behavior. *Journal of Electron Spectroscopy and Related Phenomena*, 76:121 – 126, 1995. Proceedings of the Sixth International Conference on Electron Spectroscopy.

<sup>2</sup> Yujing Ma, Horacio Coy Diaz, Jos Avila, Chaoyu Chen, Vijaysankar Kalappattil, Raja Das, Manh-Huong Phan, Tilen ade, Jos M. P. Carmelo, Maria C. Asensio, and et al. Angle resolved photoemission spectroscopy reveals spin charge separation in metallic mose2 grain boundary. *Nature Communications*, 8(1), Feb 2017.

<sup>3</sup> B.J. Kim, H. Koh, E. Rotenberg, S.J. Oh, H. Eisaki, N. Motoyama, S. Uchida, T. Tohyama, S. Maekawa, Z.X. Shen, C. Kim, and Tsukuba /Tohoku U. /Stanford U. Appl. Phys. Dept. /SLAC SSRL /Yonsei U. /Seoul Natl. U. /LBNL, ALS/KEK. Distinct spinon and holon dispersions in photoemission spectral functions from one-dimensional srcuo2. *Nature Physics*, 2, 8 2006.

<sup>4</sup> Dalila Bounoua, Romuald Saint-Martin, Ji Dai, Tobias Rdel, Shamashis Sengupta, Emmanouil Frantzeskakis, Fran-

nois Bertran, Patrick Lefevre, Franck Fortuna, Andrs F. Santander-Syro, and Loreynne Pinsard-Gaudart. Angle resolved photoemission spectroscopy study of the spin-charge separation in the strongly correlated cuprates srcuo2 and sr2cuo3 with s=0 impurities. *Journal of Electron Spectroscopy and Related Phenomena*, 225:49 – 54, 2018.

<sup>5</sup> Egger, R. and Gogolin, A. O. Correlated transport and non-fermi-liquid behavior in single-wall carbon nanotubes. *Eur. Phys. J. B*, 3(3):281–300, 1998.

<sup>6</sup> M. A. Valbuena, P. Chudzinski, S. Pons, S. Conejeros, P. Alemany, E. Canadell, H. Berger, E. Frantzeskakis, J. Avila, M. C. Asensio, T. Giamarchi, and M. Grioni. Polarization dependence of angle-resolved photoemission with submicron spatial resolution reveals emerging one-dimensionality of electrons in nbse<sub>3</sub>. *Phys. Rev. B*, 99:075118, Feb 2019.

<sup>7</sup> M. A. Valbuena, P. Chudzinski, S. Pons, S. Conejeros, P. Alemany, E. Canadell, H. Berger, E. Frantzeskakis, J. Avila, M. C. Asensio, T. Giamarchi, and M. Grioni. Emerging one-dimensionality from self-organization of electrons in nbse<sub>3</sub>, 2016.

<sup>8</sup> Ersoy Şaşıoğlu, Christoph Friedrich, and Stefan Blügel.

- Effective coulomb interaction in transition metals from constrained random-phase approximation. *Phys. Rev. B*, 83:121101, Mar 2011.
- <sup>9</sup> Aníbal Iucci, Gregory A. Fiete, and Thierry Giamarchi. Fourier transform of the  $2k_F$  luttinger liquid density correlation function with different spin and charge velocities. *Phys. Rev. B*, 75:205116, May 2007.
- <sup>10</sup> Fabian H. L. Essler and Alexei M. Tsvelik. Finite temperature spectral function of mott insulators and charge density wave states. *Phys. Rev. Lett.*, 90:126401, Mar 2003.
- <sup>11</sup> Alexander O. Gogolin, Alexander A. Nersesyan, and Alexei M. Tsvelik. *Bosonization and Strongly Correlated Systems*. Cambridge University Press, 1999.
- <sup>12</sup> P Chudzinski. Why it is so hard to detect luttinger liquids in angle resolved photo-emission spectroscopy? *Journal of Physics: Condensed Matter*, 31(10):105601, jan 2019.
- <sup>13</sup> H J Schulz. Long-range coulomb interactions in quasi-one-dimensional conductors. *Journal of Physics C: Solid State Physics*, 16(35):6769–6787, dec 1983.
- <sup>14</sup> Torsten Karzig, Leonid I. Glazman, and Felix von Oppen. Energy relaxation and thermalization of hot electrons in quantum wires. *Phys. Rev. Lett.*, 105:226407, Nov 2010.
- <sup>15</sup> Jeffrey C. Y. Teo and C. L. Kane. Critical behavior of a point contact in a quantum spin hall insulator. *Phys. Rev. B*, 79:235321, Jun 2009.
- <sup>16</sup> Strictly speaking this is what an exact analytic solution for Hubbard model tells us when hopping between chains is not extremely strong (on-chain physics dominates on-rung physics) but the numerical results for extended Hubbard models suggest that there is no qualitative modification of this spectrum as the range of interaction is changed
- <sup>17</sup> From our treatment of  $V_{eff}$  we take  $\epsilon_{||,\perp}(q_{||}) \sim (q_{||}^2 + m^2)^{-1}$  which is equivalent to a model with infinitesimally small many body gap  $m$